JACS
JOURNAL OF THE AMERICAN CHEMICAL SOCIETY

ARTICLE

pubs.acs.org/JACS

Silanones and Silanethiones from the Reactions of Transient Silylenes with Oxiranes and Thiiranes in Solution. The Direct Detection of Diphenylsilanethione.

Svetlana S. Kostina and William J. Leigh*

Department of Chemistry and Chemical Biology, McMaster University, 1280 Main Street West, Hamilton, ON Canada, L8S 4M1

Supporting Information

ABSTRACT: The transient silylenes $SiMe_2$ and $SiPh_2$ react with cyclohexene oxide (CHO), propylene oxide (PrO), and propylene sulfide (PrS) in hydrocarbon solvents to form products consistent with the formation of the corresponding transient silanones and silanethiones, respectively. Laser flash photolysis studies show that these reactions proceed via multistep sequences involving the intermediacy of the corresponding silylene−oxirane or −thiirane complexes, which are formed with rate constants close to the diffusion limit in all cases and exhibit UV absorption spectra similar to those of the corresponding complexes with the non-reactive O- and S-donors, tetrahydrofuran and tetrahydrothiophene. The $SiMe_2$-PrO and $SiPh_2$-PrO complexes both exhibit lifetimes of ca. 300 ns, and are longer-lived than the corresponding complexes with CHO, which are both in the range of 230−240 ns. On the other hand, the silylene-PrS complexes are considerably shorter-lived and vary with silyl substituent; the $SiMe_2$−PrS complex decays with the excitation laser pulse (i.e., $\tau \leq 25$ ns), while the $SiPh_2$−PrS complex exhibits $\tau = 48 \pm 3$ ns. The decay of the $SiPh_2$−PrS complex affords a long-lived transient product exhibiting $\lambda_{max} \approx 275$ nm, which has been assigned to diphenylsilanethione ($Ph_2Si{=}S$) on the basis of its second order decay kinetics and absolute rate constants for reaction with methanol, *tert*-butanol, acetic acid, and *n*-butyl amine, for which values in the range of 1.4×10^8 to 3.2×10^9 M^{-1} s^{-1} are reported. The experimental rate constants for decay of the $SiMe_2$−epoxide and −PrS complexes indicate free energy barriers ($\Delta G^{\ddagger}$) of ca. 8.5 and ≤7.1 kcal mol^{-1} for the rate-determining steps leading to dimethylsilanone and -silanethione, respectively, which are compared to the results of DFT (B3LYP/6-311+G(d,p)) calculations of the reactions of SiH_2 and $SiMe_2$ with oxirane and thiirane. The calculations predict a stepwise C−O cleavage mechanism involving singlet biradical intermediates for the silylene−oxirane complexes, and a concerted mechanism for silanethione formation from the silylene−thiirane complexes, in agreement with earlier ab initio studies of the SiH_2−oxirane and −thiirane systems.

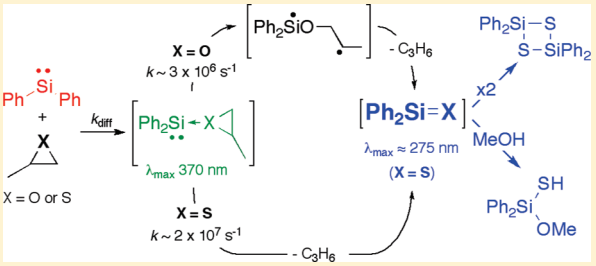

INTRODUCTION

It is well established that the chemistry of divalent silicon compounds, or silylenes, shares many common characteristics with that of singlet carbenes.[1−3] Closer scrutiny, however, usually reveals fundamental mechanistic differences between the two homologous species. For example, both species typically react rapidly with water and alcohols via net O−H insertion, yet singlet carbenes most commonly do so via a two-step mechanism involving initial protonation followed by ion-pair combination,[4] while silylenes react via initial nucleophilic attack followed by (catalytic) proton transfer.[5] The latter mechanism evidently occurs much less commonly with singlet carbenes than that involving initial protonation at the divalent center.[4,6,7] Conversely, there are few recognized examples known of silylene reactions initiated by protonation at silicon.[8,9]

A second reaction with oxygen-containing substrates that is common to both silylenes and singlet carbenes is the abstraction of oxygen from oxiranes, which yields the corresponding alkene and silanone or carbonyl compound, respectively (eq 1).[10−13] Early product- and kinetic studies of the reactions of $SiMe_2$ with the parent oxirane and various substituted derivatives were interpreted in terms of a multistep mechanism involving the initial formation of a silylene−oxirane complex.[10−12,14,15] Tzeng and Weber proposed that the collapse of the complex proceeds via a stepwise mechanism involving a zwitterionic intermediate, in order to account for the formation of siloxacyclohexenes in the reactions of $SiMe_2$ with vinyl epoxides, in addition to dimethylsilanone and the corresponding diene (eq 2).[11] Various details of the mechanism have received support from subsequent theoretical calculations,[16−18] and by recent kinetic studies of the reaction of SiH_2 with oxirane in the gas phase.[19] The analogous reaction with singlet carbenes is also thought to proceed with the

Received: September 1, 2010
Published: March 08, 2011

dx.doi.org/10.1021/ja107881p | J. Am. Chem. Soc. 2011, 133, 4377–4388

initial formation of a polar carbene−oxirane complex, or ylide.[20−22]

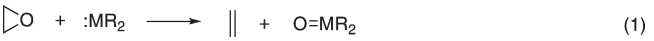

(1)

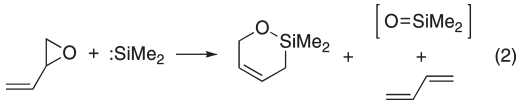

(2)

Singlet carbenes are also known to abstract sulfur from thiiranes,[22,23] doing so substantially more rapidly than O-atom abstraction from oxiranes according to the kinetic studies of Pezacki et al for several carbene systems in solution.[22] The corresponding reaction with silylenes has not yet been studied experimentally, though theory predicts the reaction should proceed with similar facility as that with oxiranes, and also via a mechanism initiated by the spontaneous formation of a Lewis acid−base complex between the silylene and the heteroatom in the substrate.[16−18]

According to the ab initio (MP2/6-31G(d,p) and QCISD/6-31G(d,p)) calculations of Apeloig and co-workers, the main mechanistic difference between the reactions of SiH_2 with oxirane and thiirane lies in the mode of collapse of the intermediate complexes, with the SiH_2−oxirane complex undergoing sequential C−O bond cleavage to yield a biradical intermediate in the initial step, and the SiH_2−thiirane complex undergoing concerted fragmentation.[16] The calculations predict that dissociation of the complex is the rate-controlling step in both cases, and proceeds with similar free energy barriers. Two subsequent DFT studies[17,18] afforded results that were in reasonable general agreement with those of the earlier ab initio study, but failed to locate the biradical intermediate in the decomposition of the SiH_2−oxirane complex that was found by Apeloig and Sklenak.[16] As a result, concerted asynchronous cleavage mechanisms were predicted for both the oxirane- and thiirane-complexes, the latter via a lower enthalpic barrier than the former.[17,18] Similar energetics and mechanisms were predicted for the corresponding reactions of $SiMe_2$ with oxirane and thiirane.[18]

These reactions represent a potentially useful method for the photochemical synthesis of transient silanone and silanethione derivatives, for study of their reactivities in solution by time-resolved spectroscopic methods. Remarkably little quantitative information on the reactivity of these species exists, in spite of considerable interest over the past few decades in the chemistry of silicon-chalcogen double bonds[24−27] and the synthesis of stable compounds containing these intrinsically highly reactive moieties.[28−44] Several stable silacarbonyl compounds have been reported,[30−36] all but one of them[31] containing chelating ligands to stabilize the highly reactive silicon−oxygen double bond. However, a stable dialkyl- or diarylsilanone (with or without chelating ligands) has yet to be reported, and thus, most of our knowledge regarding the spectroscopic properties and structures of these compounds has been gained through low-temperature matrix isolation studies[13,24,25,45−50] and theoretical calculations.[26,48,51−58] Silanethiones are thought to be more thermodynamically stable than silanones due to a lower polarity of the Si═S bond,[26,51,59] and indeed two sterically stabilized, base-free silanethiones have been reported[41−44] in addition to a few donor-coordinated derivatives.[36−38] However, remarkably few transient silanethiones have been observed directly, either in low-temperature matrixes,[60] the gas phase,[61−63] or in solution.[40]

In the present paper, we report the results of kinetic and product studies of the reactions of the transient silylenes $SiMe_2$ and $SiPh_2$ with cyclohexene oxide (CHO), propylene oxide (PrO), and propylene sulfide (PrS) in hexanes solution. The goals of the study were to investigate and compare the reactions of these silylenes with simple oxiranes and thiiranes and determine the kinetics and mechanisms as completely as possible, to see whether the intermediate complexes proposed in earlier studies could be detected and characterized kinetically, and to attempt to detect the resulting (diaryl) silanones and silanethiones directly and study their reactivities in a quantitative way. As in our previous studies of these two transient silylenes in solution,[5,64,65] they were generated and detected by laser photolysis of the corresponding oligosilane derivatives **1** and **2**, respectively. The well-known acyclic $SiPh_2$-precursor, trisilane **3**,[66−70] was also employed in some of the product studies. We have also carried out a density functional theory (DFT) study of the reactions of SiH_2 and $SiMe_2$ with oxirane and thiirane, and compare the results to the experimental data for $SiMe_2$.

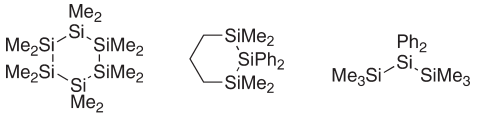

1 2 3

RESULTS

Laser Flash Photolysis Experiments. Laser flash photolysis experiments were carried out with rapidly flowed, deoxygenated solutions of **1** (ca. 4×10^{-4} M) and **2** (ca. 6×10^{-5} M) in anhydrous hexanes at 25 ± 1 °C using the pulses from a KrF excimer laser (248 nm, 90−105 mJ, ca. 20 ns) for excitation. The silylenes are observed as promptly formed transients with UV−vis absorption bands centered at λ_{max} = 465 nm ($SiMe_2$; $\tau \approx 500$ ns) and λ_{max} = 300 and 515 nm ($SiPh_2$; $\tau \approx 1.7$ μs), and in the absence of added substrates decay with the concomitant formation of longer-lived UV−vis absorptions due to the corresponding disilenes, Si_2Me_4 (λ_{max} = 360 nm, $\tau \approx 20$ μs) and Si_2Ph_4 (λ_{max} = 290 and 460 nm, $\tau \approx 100$ μs), respectively.[5,64,65] Silylene formation from **2** is accompanied by the formation of minor amounts (ca. 3%) of silene **4**, which gives rise to long-lived residual absorptions centered at 460 nm on which the spectra due to $SiPh_2$ and Si_2Ph_4 are superimposed.[64,70] This species exhibits much lower reactivity than $SiPh_2$ toward most substrates, so its presence in the photolysis mixture does not compromise the determination of rate constants or the characterization of transient products from the reactions of the silylene with added substrates.

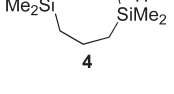

4

Addition of CHO (0.1−1.5 mM) to hexanes solutions of **1** resulted in shortening of the lifetime of the silylene, suppression of the formation of Si_2Me_4, and the appearance of a new transient species giving rise to absorptions centered at λ_{max} = 310 nm. The

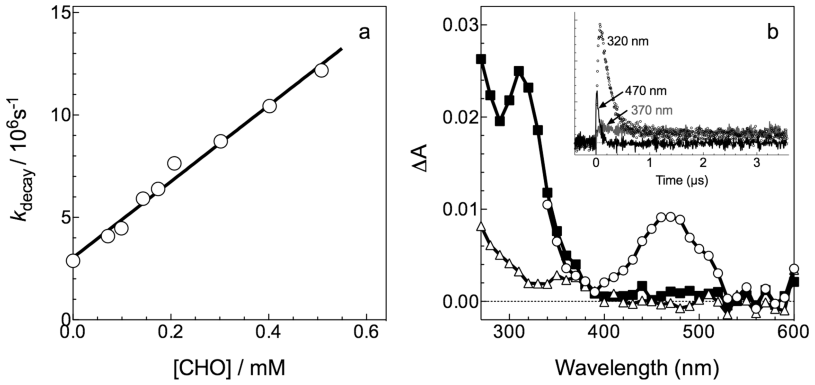

Figure 1. (a) Plot of the pseudo-first-order decay coefficient (k_{decay}) of the $SiMe_2$ absorption at 470 nm vs [CHO]. (b) Transient absorption spectra from laser flash photolysis of a hexanes solution of **1** containing 1 mM CHO, recorded 26−38 ns (○), 128−154 ns (■), and 1.49−1.51 μs (Δ) after the laser pulse (the portion of the 26−38 ns spectrum below 340 nm is distorted due to sample fluorescence and is not shown); the inset shows transient absorbance vs time profiles recorded at 320, 370, and 470 nm.

latter grew in on a similar time scale as the silylene decay at low CHO concentrations, both its growth rate and maximum intensity increasing with increasing CHO concentration over the 0.2−1.5 mM range. The bimolecular rate constant for its formation from free $SiMe_2$ and CHO was determined from the slope of a plot of the pseudo-first-order decay rate coefficients for decay of the silylene absorption (k_{decay}) versus CHO concentration according to the expression of eq 3, where Q denotes the substrate, k_Q is the bimolecular rate constant for its reaction with the free silylene, and k_0 is the apparent pseudo-first-order rate coefficient for silylene decay in the absence of added substrate. The plot (see Figure 1a) showed excellent linearity, and exhibited a slope of $k_Q = (1.9 \pm 0.2) \times 10^{10}\ M^{-1}\ s^{-1}$. The value is the same within experimental error to that for reaction of free $SiMe_2$ with THF under similar conditions ($k = (1.7 \pm 0.2) \times 10^{10}\ M^{-1}\ s^{-1}$ in hexanes at 25 °C).[65]

$$k_{decay} = k_0 + k_Q[Q] \qquad (3)$$

The transient product decayed with first-order kinetics, exhibiting a lifetime (τ = 230 ± 12 ns) that was independent of CHO concentration up to at least 0.17 M (see Figure S1). Figure 1b shows a series of transient absorption spectra recorded for **1** in the presence of 1 mM CHO, where the lifetime of $SiMe_2$ is reduced to ca. 60 ns and the spectrum of the 310 nm species grows in to achieve its maximum intensity ca. 75 ns after the laser pulse. The spectrum of the latter species is typical of $SiMe_2$-*O*− donor complexes such as those with THF and aliphatic alcohols under similar conditions,[5,65,71] and is thus assigned to the $SiMe_2$−CHO complex.

Lifetime quenching of $SiMe_2$ by propylene oxide (PrO) was equally efficient ($k_Q = (1.6 \pm 0.2) \times 10^{10}\ M^{-1}\ s^{-1}$) and also led to the formation of a single product absorption centered at λ_{max} = 310 nm (Figure S2), which can be assigned to the $SiMe_2$−PrO complex. The species decayed with clean first-order kinetics and lifetime τ = 325 ± 20 ns, the average of several measurements over the 0.005−0.093 M concentration range in added PrO (Figure S1).

The formation of Si_2Me_4 is completely quenched in the presence of CHO or PrO at concentrations of ca. 2 mM or higher, indicating that irreversible reaction is responsible for the decay of the $SiMe_2$−oxirane complexes, and that it proceeds with a rate constant considerably greater than reversion of the complex back to the free silylene and substrate. Only very weak residual absorptions remained after the complexes decayed, indicating that the products of decomposition of the complexes do not absorb significantly in the 270−600 nm range of the spectrum.

Efficient reductions in the lifetime of $SiMe_2$ and suppression of the formation of Si_2Me_4 were also observed upon addition of PrS to hexanes solutions of **1**; a bimolecular rate constant of $k_Q = (2.1 \pm 0.2) \times 10^{10}\ M^{-1}\ s^{-1}$ for the primary reaction with the silylene was determined from the slope of a linear plot of k_{decay} versus [PrS] according to eq 3 (see Figure S3a). A transient spectrum recorded in the presence of 5 mM PrS (Figure S3b) showed evidence of new, very short-lived transient absorptions centered at $\lambda_{max} \approx 320$ nm ($\tau \leq 25$ ns), though they were difficult to detect reproducibly due to interference from strong sample fluorescence in the 280−330 nm range of the spectrum. The species is assigned to the $SiMe_2$−PrS complex, the expected spectrum of which was established using tetrahydrothiophene (THT) as a representative *S*-donor; this substrate reacts with $SiMe_2$ with the same rate constant as that for PrS (see Figure S4a), and results in the formation of a relatively long-lived transient with UV-absorption maximum centered at λ_{max} = 325 nm ($\tau > 10$ μs; Figure S4b). The spectrum agrees well with that reported by Shizuka and co-workers in cyclohexane,[72] who assigned it to the $SiMe_2$−THT complex. The decay of the $SiMe_2$−THT complex is accompanied by the growth of the characteristic absorptions due to Si_2Me_4 (λ_{max} = 370 nm), which were quite prominent at low (0.2−2.0 mM) THT concentrations but then decreased modestly as the concentration was increased to higher levels, probably due to the presence of low concentrations of reactive impurities in the solvent and/or substrate. In contrast, the formation of Si_2Me_4 is completely quenched in the presence of PrS, indicating that irreversible reaction is responsible for the rapid decay of the $SiMe_2$−PrS complex. Again, the products of this reaction do not absorb sufficiently strongly in the 270−600 nm wavelength range for us to detect them by time-resolved UV−vis spectroscopy.

Addition of CHO, PrO, or PrS to hexanes solutions of **2** caused similar behavior as was observed in the corresponding experiments with **1**; the decay of the $SiPh_2$ absorption (monitored at 530 nm) was accelerated in the presence of added substrate, the signal decayed completely to baseline with clean first-order kinetics, and formation of the silylene dimer (Si_2Ph_4; λ_{max} = 460 nm) was suppressed, all to an increasing extent with

dx.doi.org/10.1021/ja107881p |*J. Am. Chem. Soc.* 2011, 133, 4377–4388

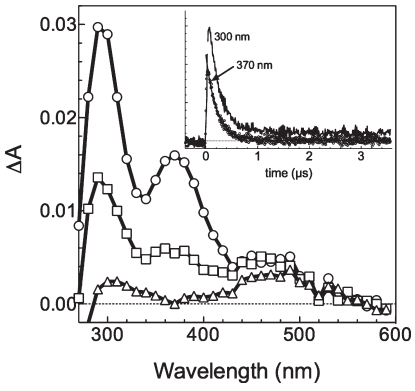

Figure 2. Transient absorption spectra recorded 65−77 ns (○), 0.27−0.29 μs (□), and 3.50−3.57 μs (Δ) after the laser pulse, by laser flash photolysis of a deoxygenated hexanes solution of **2** containing 17.0 mM CHO; the inset shows transient decay/growth profiles recorded at 300 and 370 nm. The weak residual absorption centered at ca. 460 nm is due to the long-lived photolysis coproduct, silene **4**.

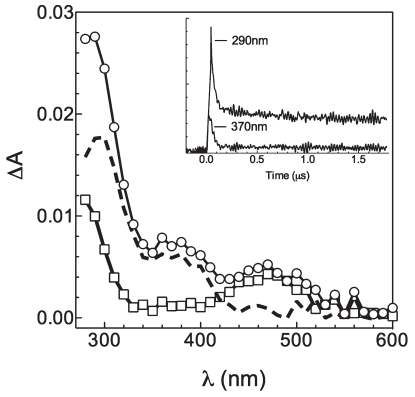

Figure 3. Transient absorption spectra recorded 48−54 ns (○) and 0.70−0.72 μs (□) after the laser pulse, by laser flash photolysis of a deoxygenated hexanes solution of **2** containing 4.7 mM PrS; the dashed line shows the difference spectrum, constructed by subtracting the 0.70 μs spectrum from the 48 ns spectrum. The inset shows transient decay/growth profiles recorded at 290 and 370 nm.

increasing substrate concentration. Plots of k_{decay} for the silylene absorption versus [Q] were linear in all three cases (Figures S5−S7), and afforded bimolecular rate constants in the range of $(1.1-1.2) \times 10^{10}$ M^{-1} s^{-1}. With all three substrates, the decay of the silylene was accompanied by the growth of a transient product with absorption bands centered at $\lambda_{max} \approx 290$ and 370 nm, which (at higher substrate concentrations) decayed with a first-order rate constant that was independent of substrate concentration (Figure S8).

Figure 2 shows transient absorption spectra and representative absorbance-time profiles obtained with hexanes solutions of **2** containing 17 mM CHO; the corresponding spectra with PrO as substrate (Figure S9) were virtually identical. The spectra are in both cases indistinguishable from those of the $SiPh_2$−THF complex under similar conditions,[65] allowing their assignment to the corresponding $SiPh_2$−oxirane complexes. The lifetime of the $SiPh_2$−CHO complex (τ = 240 ± 10 ns) was modestly shorter than that of the $SiPh_2$−PrO complex (τ = 295 ± 15 ns), as found for the corresponding $SiMe_2$−oxirane complexes (vide supra). Again, no new products absorbing in the 270−600 nm range arising from the decay of the complexes could be detected in either case.

Laser photolysis of optically matched solutions of **2** containing ca. 10 mM CHO and ca. 10 mM THF, under conditions of equal laser intensity, revealed the maximum absorbance at 365 nm to be ca. 25% lower for the $SiPh_2$−CHO complex than for the $SiPh_2$−THF complex. Kinetic simulations showed the value to be within the range expected given the difference in the decay kinetics of the two species, assuming equal extinction coefficients at the monitoring wavelength. Provided the assumption of equal extinction coefficients is valid, this shows that the lower peak intensity observed for the $SiPh_2$−CHO complex (τ = 240 ± 10 ns) is due entirely to its much more rapid *decay* compared to that of the $SiPh_2$−THF complex (τ > 20 μs), and not to the presence of a second, undetectable reaction channel that competes with the formation of the complex from the free silylene and the oxirane. Thus, complexation of the free silylene proceeds *quantitatively* in the presence of both O-donor substrates at concentrations of 10 mM.

Transient UV−vis spectra recorded by laser photolysis of a hexanes solution of **2** containing 4.7 mM PrS (Figure 3) showed clear evidence for the formation of *two* transient products of the reaction of $SiPh_2$ with the thiirane: a short-lived one exhibiting absorption bands centered at ca. 300 and 370 nm and lifetime τ = 48 ± 8 ns, and a second, much longer-lived one that is detected as a tail absorption at the blue edge of the spectral window, in the range which is normally dominated by the bleaching signal due to the precursor (e.g., see Figure 2). The shorter-lived species is assigned to the $SiPh_2$−PrS complex, based on comparisons of its spectrum to that recorded with a solution of **2** in hexanes containing 5.3 mM THT (Figure S10). It should be noted that the long-lived species present at the end of the decay of the $SiPh_2$−PrS complex is *different* from the one observed in the presence of THT, which complexes strongly with $SiPh_2$ but does not inhibit the formation of the dimer (Si_2Ph_4; λ_{max} = 460 nm) and higher oligomerization products that form over a more extended time scale. The latter also give rise to strong long-lived absorptions at the blue edge of our spectral window, and are also formed in the presence of THF.[5,65]

Table 1. Absolute Rate Constants (k_Q, in Units of 10^9 M^{-1} s^{-1}) for Quenching of $SiMe_2$ and $SiPh_2$ by Cyclohexene Oxide (CHO), Propylene Oxide (PrO), Propylene Sulfide (PrS), and Tetrahydrothiophene (THT). and First-Order Rate Constants for Decay of the Resulting Complexes (k_{cplx}, in Units of 10^6 s^{-1}) in hexanes at 25 ± 1 °C[a]

	$SiMe_2$		$SiPh_2$	
substrate	$k_Q/10^9$ M^{-1} s^{-1}	$k_{cplx}/10^6$ s^{-1}	$k_Q/10^9$ M^{-1} s^{-1}	$k_{cplx}/10^6$ s^{-1}
CHO	19 ± 2	4.3 ± 0.3	10.0 ± 0.4	4.2 ± 0.3
PrO	16 ± 2	3.1 ± 0.2	12 ± 2	3.4 ± 0.2
PrS	21 ± 2	≥40 ± 4	11.2 ± 0.4	18 ± 3
THT	21 ± 2	<0.5[b]	15 ± 2	<0.5[b]

[a] Errors in k_Q-values are reported as twice the standard error from linear least-squares analysis of plots of silylene k_{deccay} values vs [Q] according to eq 1. The k_{cplx}-values and their uncertainties are reported as the average and standard deviation of 9−13 independent determinations. [b] Decay is second order.

Table 1 lists the absolute rate constants determined in this work for quenching of $SiMe_2$ and $SiPh_2$ by CHO, PrO, PrS, and THT in hexanes at 25 ± 1 °C, along with the first-order decay

dx.doi.org/10.1021/ja107881p | J. Am. Chem. Soc. 2011, 133, 4377–4388

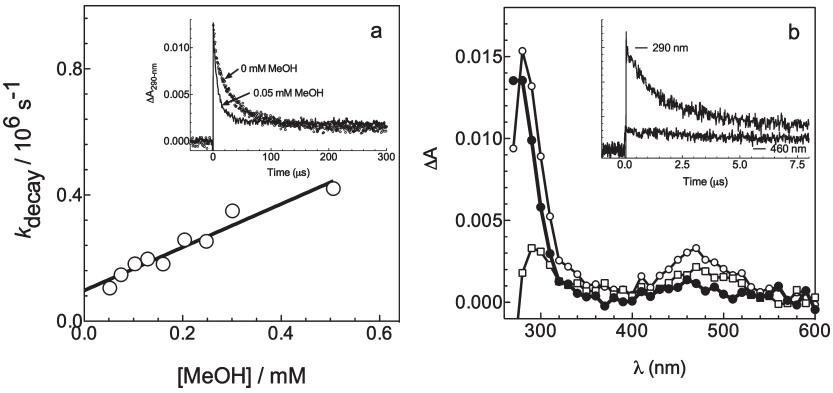

Figure 4. (a) Plot of the pseudo-first-order decay coefficient (k_{decay}) of the 290 nm absorption observed from **2** in the presence of PrS (20 mM) and MeOH (0.05−0.5 mM) vs [MeOH]; the inset shows transient decays recorded in the presence of 0 and 0.05 mM MeOH. (b) Transient absorption spectra recorded 0.18−0.24 (○) and 8.56−8.72 μs (□) after the laser pulse, by laser flash photolysis of deoxygenated hexanes solution of **2** containing 20 mM PrS and 0.5 mM MeOH; the inset shows transient decays recorded at 290 and 460 nm. The third spectrum (●) was calculated by subtraction of the 8.56−8.72 μs spectrum from the 0.18−0.24 μs spectrum.

Table 2. Absolute second-Order Rate Constants (k_Q in Units of 10^9 M^{-1} s^{-1}) for Quenching of the Long-Lived Transient Product of the Reaction of $SiPh_2$ with PrS by MeOH, *t*-BuOH, AcOH, and *n*-$BuNH_2$ in Hexanes Containing 0.02 M PrS at 25 ± 1 °C[a]

substrate	MeOH	*t*-BuOH	AcOH	*n*-$BuNH_2$
$k_Q/10^9$ M^{-1} s^{-1}	0.85 ± 0.09[b]	0.14 ± 0.01	3.2 ± 0.7	2.1 ± 0.1

[a] Unless otherwise noted, errors are reported as twice the standard error from linear least-squares analysis of plots of k_{decay} values vs [Q] according to eq 3. [b] The average and standard deviation of two independent determinations.

rate constants of the resulting Lewis acid−base complexes. The latter are reported as the average of 9−13 independent determinations in each case.

Experiments with **2** and PrS carried out on longer time scales revealed that the long-lived absorptions formed in the reaction of $SiPh_2$ with PrS are also transient, decaying over roughly 100 μs with approximate second-order kinetics ($2k/\varepsilon_{290\text{-nm}}$ = (2.3 ± 0.2) × 10^6 cm s^{-1}; see Figure S11). Addition of submillimolar amounts of MeOH (to hexanes solutions of **2** containing 20 mM PrS) resolved the absorption into two components, consisting of a first-order decay superimposed on a weak, nondecaying residual absorption. The decay rate of the main component increased with increasing methanol concentration, and a plot of k_{decay} versus [MeOH] was linear with slope k_{MeOH} = (8.5 ± 0.9) × 10^8 M^{-1} s^{-1}, the average of two independent determinations. Figure 4a shows the plot of k_{decay} versus [MeOH] that was obtained in one experiment. Similar results were obtained upon addition of *tert*-butanol (*t*-BuOH; 0.2−1.5 mM), acetic acid (AcOH; 0.05−0.5 mM), or *n*-butyl amine (*n*-$BuNH_2$; 0.1−1.5 mM). The quenching plots are shown in Figure S12, while the corresponding second-order rate constants are listed in Table 2. The weak residual absorption that was observed in these experiments may be due to direct photolysis of PrS, which absorbs weakly at the excitation wavelength ($\varepsilon_{248\text{-nm}}$ = 23 M^{-1} cm^{-1}); laser photolysis of a 10 mM hexanes solution of PrS gives rise to similarly weak, nondecaying absorptions in the 270−290 nm range of the spectrum, which is consistent with this interpretation. It should be noted that the relative concentrations of PrS and secondary substrate in these experiments are such that reaction with PrS remains the dominant mode of decay of the free silylene.

As indicated above, the raw UV/vis spectra shown in Figure 3 contain contributions from those of silene **4** and the precursor bleaching signal, superimposed on the spectrum of the long-lived product of the reaction of $SiPh_2$ and PrS. Figure 4b shows transient spectra recorded over a longer time scale with a solution of **2** containing 0.02 M PrS and 0.5 mM MeOH, and the difference spectrum obtained by subtraction of the spectrum remaining at the end of the decay of the long-lived product from that at the beginning of the decay. The difference spectrum shows that the long-lived product of the reaction of $SiPh_2$ with PrS exhibits a strong absorption band centered at $\lambda_{max} \approx 275$ nm and (perhaps) a secondary long wavelength band centered at $\lambda_{max} \approx 460$ nm, though the latter is very weak and should be accepted with caution. We assign the species to diphenylsilanethione ($Ph_2Si{=}S$) on the basis of its UV−vis spectrum and kinetic behavior.

Product Studies. A series of steady-state photolysis experiments were carried out in order to determine the ultimate products of the reactions of $SiMe_2$ and $SiPh_2$ with CHO, PrO, and PrS, and their chemical yields relative to consumed silylene precursor and/or substrate. The experiments were carried out in quartz NMR tubes containing deoxygenated cyclohexane-d_{12} solutions of **1** or **2** (0.05 M), the substrate (0.1−0.2 M), and internal standard (dioxane and/or Si_2Me_6; ca. 0.01 M), both in the absence and presence of added D_3 (0.2 M) as a scavenger for the expected silanones and silanethiones. The solutions were irradiated with 254 nm light, following the course of the photolyses by ^{1}H NMR spectroscopy and/or GC/MS over the 0 to ca. 10% conversion range in silylene precursor. Products were identified in the crude photolysis mixtures by comparison of their (^{1}H and ^{29}Si) NMR and mass spectral characteristics to literature data or to those of independently prepared authentic samples. Product yields were determined relative to consumed precursor and/or substrate from the relative slopes of concentration versus time plots, constructed from the ^{1}H NMR integrals for as many of the components of the mixtures as was practically possible. This was confined to the alkene relative to consumed substrate in the experiments with **1** because the overlap of the ^{1}H NMR resonances due to **1** and its photoproducts make it impossible to follow the consumption of the precursor by this analytical method; more complete quantitation of the photolyses was possible

dx.doi.org/10.1021/ja107881p |*J. Am. Chem. Soc.* 2011, 133, 4377–4388

in the experiments with **2**. The results of the experiments with **1** and CHO were analogous to those reported previously by Goure and Barton in their early study of the photolysis of **1** in the presence of cyclooctene oxide,[10] and are described in the Supporting Information. The results of the other experiments are summarized below, while representative NMR spectra and concentration versus time plots are shown in the Supporting Information.

Photolysis of **1** in the presence of propylene sulfide (PrS) and D_3 afforded as the major products pentamethylcyclopentasilane (**5**), propene (**6**), and compound **7**, the product of formal insertion of $Me_2Si{=}S$ into D_3,[73,74] along with smaller amounts of compound **8** from competing reaction of $SiMe_2$ with D_3[75] (eq 4 and Figures S15, S16). A variety of other minor products containing $SiMe_2$ moieties were also formed in the photolysis (see Figure S16), but none of them could be identified.

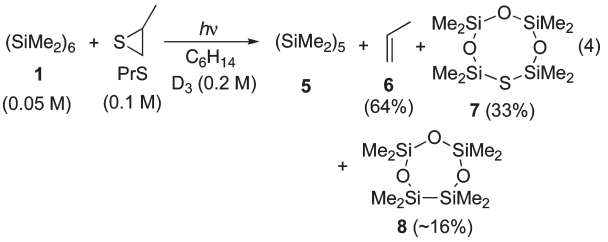

Photolysis of **2** in the presence of PrO and D_3 afforded **6**, disilacyclopentane **9**,[64] and cyclotetrasiloxane **10**[76] as the major products (eq 5; Figures S17, S18). Compound **11**, arising presumably from insertion of $SiPh_2$ into a Si−O bond of D_3, was also detected in trace amounts by GC/MS and was tentatively assigned on the basis of its mass spectrum. The aromatic region of the ^{1}H NMR spectrum of the photolysate exhibited broad underlying absorptions, suggesting the formation of oligo- or polymeric material. Support for the structural assignment of **11** was obtained by photolyzing a deoxygenated 0.05 M hexanes solution of **2** containing only D_3 (0.2 M), which showed the same compound to be formed as the major $SiPh_2$-containing product. Photolysis of **2** and PrO in the absence of D_3 led to the formation of **6** (51 ± 2%), **9** (92 ± 3%), and significantly greater amounts of oligo- or polymeric material than were obtained in the presence of D_3 (Figure S19).

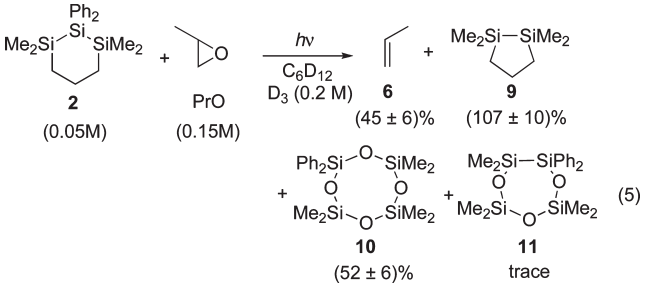

Photolysis of **2** in the presence of PrS afforded **6**, **9** and tetraphenylcyclodisilthiane (**12**) as the major products (eq 6 and Figure S20a). Compound **12** was identified by spiking the photolysis mixture with an authentic sample.[77] A similar mixture of products was obtained upon photolysis of **2** and PrS in the presence of D_3 (Figures S20b, S21); while trace amounts of compound **11** were also detected in the photolysate by GC/MS, no evidence for the formation of compound **13**, the anticipated product of reaction of $Ph_2Si{=}S$ with D_3,[78] could be obtained.

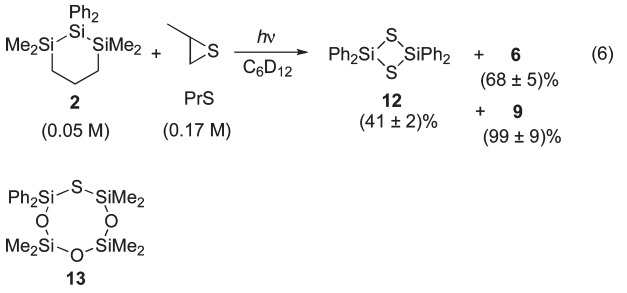

Finally, a solution of **2** (0.05 M), PrS (0.08 M), and MeOH (0.005 M) in C_6D_{12} was photolyzed in an attempt to trap the silanethione as the methanol adduct. Indeed, the ^{1}H NMR spectra of the photolyzed mixture showed evidence for the formation of two methoxyl-containing products (eq 7; Figure S22, S23). The minor of these was identified as methoxydiphenylsilane (**14**) by spiking the mixture with an authentic sample, while the major one was identified as methoxydiphenylsilanethiol (**15**) on the basis of NMR and mass spectral data. The characteristic aromatic resonances of the silanethione dimer (**12**) could not be detected in this experiment.

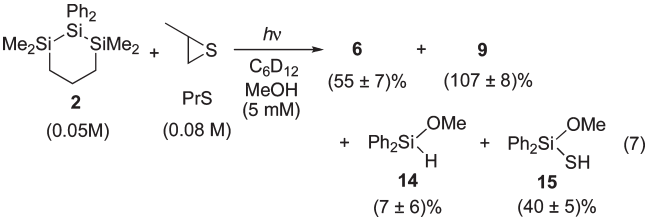

Computational Studies. The thermochemical parameters associated with the formation and first step in the decomposition of the complexes of SiH_2 and $SiMe_2$ with oxirane and thiirane were modeled using density functional theory, employing the B3LYP exchange-correlation functional[79,80] in conjunction with the standard 6-311+G(d,p) basis set. Starting structures for geometry-optimization of the complexes and the transition states for their decomposition were constructed using key geometric parameters taken from the earlier ab initio study of the SiH_2−oxirane and −thiirane systems by Apeloig and Sklenak.[16] The transition states were initially optimized using the restricted procedure, and then reoptimized using the unrestricted procedure with HOMO−LUMO mixing in the initial guess leading to unrestricted wave functions. This had, at most, only very minor effects on the energies and geometries of the transition structures compared to the results obtained using the restricted procedure without HOMO−LUMO mixing. Intrinsic Reaction Coordinate (IRC) calculations starting at the saddle points were carried out in the reverse direction to verify the connections between the transition structures and the complexes, and in the forward direction to establish starting structures for the final geometry-optimizations of the primary decomposition products; these calculations were carried out using the unrestricted procedure with HOMO−LUMO mixing in all cases, as were the final geometry optimizations and frequencies calculations for the biradicals. All minima and transition states were characterized by their vibrational frequencies. The reported thermodynamic

dx.doi.org/10.1021/ja107881p |J. Am. Chem. Soc. 2011, 133, 4377–4388

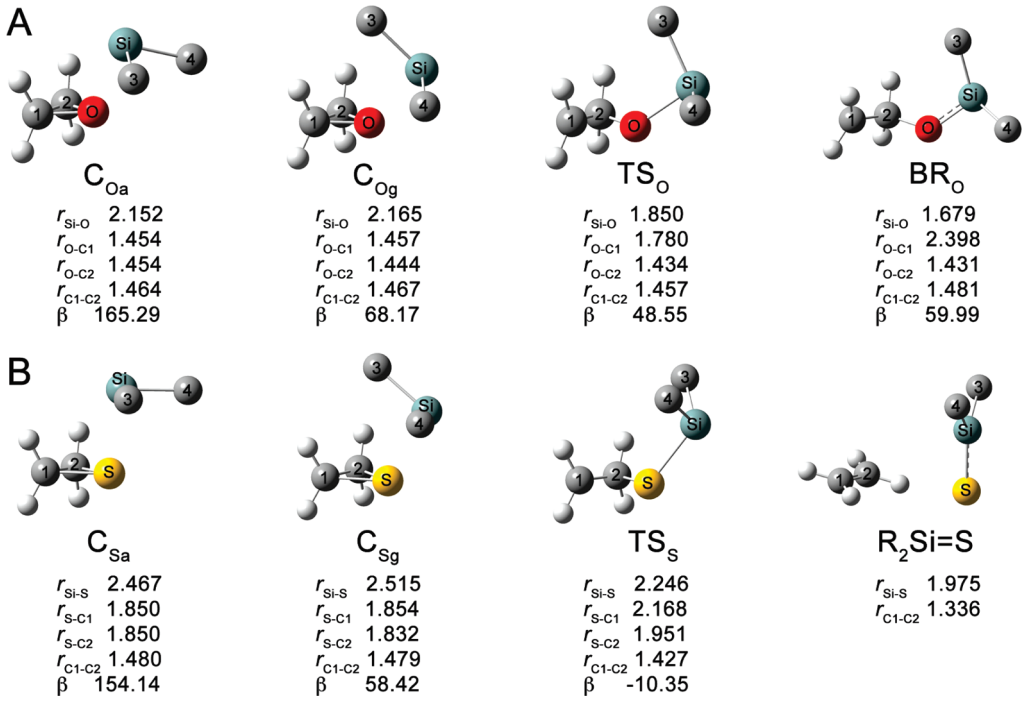

Figure 5. Calculated (B3LYP/6-311+G(d,p)) structures and selected bond distances (in Å) and angles (in degrees) of the anti and gauche conformers of the (A) $SiMe_2$−oxirane and (B) $SiMe_2$−thiirane complexes ("C_X"), the transition states for C-X bond cleavage of the gauche conformers ("TS_X"), and the first-formed products of the reaction; "β" denotes the C3−Si−X−C2 dihedral angle. The methyl-hydrogens have been omitted from the structures for clarity.

Table 3. Calculated (B3LYP/6-311+G(d,p)//B3LYP/6-311+G(d,p)) Standard Enthalpies (ΔH_{298}) and Free Energies (ΔG_{298}) of Stationary Points on the Potential Energy Surfaces for Reaction of SiH_2 and $SiMe_2$ with Oxirane and Thiirane, in kcal mol^{-1} Relative to the Energies of the Reactive Gauche Conformers of the Corresponding Silylene−Substrate Complexes

	SiH_2 + oxirane		$SiMe_2$ + oxirane		SiH_2 + thiirane		$SiMe_2$ + thiirane	
	ΔH_{298}	ΔG_{298}	ΔH_{298}	ΔG_{298}	ΔH_{298}	ΔG_{298}	ΔH_{298}	ΔG_{298}
Free Reactants	+14.8	+4.4	+7.2	−4.0	+18.0	+7.8	+8.0	−3.4
anti-Complex	+0.6	+0.1	−1.6	−1.6	−1.2	−1.2	−2.0	−2.2
Transition State	+8.8	+9.2	+5.6	+6.6	+6.5	+5.9	+3.2	+3.5
Biradical	−11.1	−13.0	−18.4	−19.5	−	−	−	−
$R_2Si{=}X + C_2H_4$	−42.7	−54.2	−57.2	−67.8	−30.2	−41.4	−44.7	−57.0

data (vide infra) are given at 298.15 K from unscaled vibrational frequencies in the harmonic approximation.

Figure 5 shows the calculated (B3LYP/6-311+G(d,p)) structures of the Lewis acid−base complexes of $SiMe_2$ with oxirane and thiirane, the transition states for C−X bond cleavage from the reactive gauche conformers of the complexes, and the primary products of these reactions.

Dissociation of the gauche SiR_2−oxirane complexes led to the corresponding $R_2SiOCH_2CH_2$ biradicals, while dissociation of the SiR_2−thiirane complexes led directly to ethylene and the corresponding silanethione, in general agreement with Apeloig's and Sklenak's ab initio results for the SiH_2−oxirane and −thiirane systems.[16] As expected, two low-energy conformers were found for each of the complexes, one with the silylene substituents oriented anti to the oxirane or thiirane ring and the other with the substituents in a gauche arrangement. In all cases except for the SiH_2−oxirane complex, the anti conformer is lower in free energy, by an amount ranging from 1.2 kcal mol^{-1} for the SiH_2−thiirane complex to 1.6 and 2.2 kcal mol^{-1} for the $SiMe_2$−complexes with oxirane and thiirane, respectively, at the B3LYP/6-311+G(d,p) level of theory; the gauche and anti conformers of the SiH_2−oxirane complex are roughly equal in energy. In any event, in each case the two conformers can be expected to be in rapid equilibrium at 25 °C, with only small barriers for their interconversion. Table 3 lists the B3LYP/6-311+G(d,p) standard enthalpies and free energies of the various species investigated, in each case relative to that of the reactive gauche conformer of the silylene−substrate complex.

Geometry optimization of the $H_2SiOCH_2CH_2$ biradical at the UMP2(full)/6-31G(d,p) and UQCISD(full)/6-31G(d,p) levels of theory with HOMO−LUMO mixing afforded significantly different structures and energies for the species than those obtained using the restricted procedure without orbital mixing.[16] Both levels of theory afforded a transoid biradical structure with a Si−O−C−C torsional angle of ca. 164°, with total electronic energies of $\Delta E = -5.2$ kcal mol^{-1} (UMP2) and −6.5 kcal mol^{-1} (UQCISD) relative to the gauche SiH_2−oxirane complex. These values, along with the zpe and thermal corrections obtained from

dx.doi.org/10.1021/ja107881p |*J. Am. Chem. Soc.* 2011, 133, 4377–4388

a frequencies calculation at the UMP2/6-31G(d,p) level, afforded standard free energy values of ΔG_{298} = −8.6 and −9.9 kcal mol^{-1}, respectively. Full details of these calculations are reported in the Supporting Information. In contrast, optimization using the restricted procedure affords a gauche geometry in both cases ($\angle_{Si-O-C-C} \approx 120°$ (MP2) and 94° (QCISD)) and corresponding energies of ΔE = −0.6 and +9.1 kcal mol^{-1} at the MP2 and QCISD levels, as reported earlier.[16] As was found with the B3LYP calculations, use of the unrestricted procedure had no effect on the structure or energy of the transition state linking the complex and the biradical, compared to those obtained using the restricted procedure. Further exploration of the model chemistry of the silylene-oxirane derived biradicals is beyond the scope of the present work.

DFT calculations were also carried out for the SiH_2− and $SiMe_2$−oxirane systems at the (U)B3LYP/6-311G(d) level of theory (Table S1); the geometries and ΔE_o-values of the gauche complexes, transition states, and final products ($R_2Si{=}O$ + ethylene) relative to the free reactants are nearly identical in every case to those reported previously by Su.[18] These calculations afforded more negative complexation free energies (by ca. 2 kcal mol^{-1}) and more positive free energies for the transition states (by ca. 0.5 kcal mol^{-1}), biradicals (by 1 to 2 kcal mol^{-1}), and final products (by 0.5−2.4 kcal mol^{-1}) compared to the corresponding calculations employing the 6-311+G(d,p) basis set. Geometry optimizations and frequencies calculations were also carried out at the B3LYP/6-311G(d) level of theory for $SiPh_2$, $Ph_2Si{=}O$, $Me_2Si{=}S$, and $Ph_2Si{=}S$ (Table S2), affording overall enthalpies of reaction of −61.8 kcal mol^{-1} for $SiPh_2$ + oxirane, −51.5 kcal mol^{-1} for $SiMe_2$ + thiirane, and −49.4 kcal mol^{-1} for $SiPh_2$ + thiirane.

Time-dependent calculations, again at the B3LYP/6-311G(d) level of theory, afforded predicted UV−vis absorption maxima of 530 nm (f 0.026; n → p) and 309 nm (f 0.244; $\pi \rightarrow \pi^*$) for $SiPh_2$, 317 nm (f 0.001; n → π^*) and 254 nm (f 0.070; $\pi \rightarrow \pi^*$) for $Ph_2Si{=}O$, and 421 nm (f 0.002; n → π^*), 305 (f 0.160; $\pi \rightarrow \pi^*$), 275 nm (f 0.160; $\pi \rightarrow \pi^*$), and 269 nm (f 0.086; $\pi \rightarrow \pi^*$) for $Ph_2Si{=}S$. The three short-wavelength ($\pi \rightarrow \pi^*$) transitions in the calculated spectrum of $Ph_2Si{=}S$ overlap to form a single, slightly asymmetric band centered at $\lambda_{max} \approx 280$ nm in the simulated spectrum, in excellent agreement with that assigned to the molecule in our laser photolysis experiments (vide supra). The calculated spectrum of $SiPh_2$ is also in outstanding agreement with the experimental (solution phase) spectrum.[64]

DISCUSSION

The product studies demonstrate that $SiPh_2$ reacts with simple oxirane derivatives in solution to afford the corresponding alkene and products consistent with the formation of diphenylsilanone ($Ph_2Si{=}O$), in an analogous fashion to $SiMe_2$ under similar conditions (vide supra and ref 10). The relative yields of alkene and D_3-trapping products in the photolyses of **1** and **2** in the presence of the oxiranes and D_3 are close to 1:1 in all cases, indicating that both transient silanones are trapped by the oligosiloxane with close to 100% efficiency under the conditions of our experiments. It is also apparent that the reactions of $SiMe_2$ and $SiPh_2$ with CHO and PrO all proceed with similar efficiencies under comparable experimental conditions, in terms of the chemical yields of alkene and silanone-derived products relative to consumed silylene precursor and/or oxirane derivative. These efficiencies are considerably less than 100%, indicating the presence of additional reaction pathways involving the silylenes and the oxiranes that we have been unable to characterize completely.

The study also provides the first experimental demonstration of the homologous reactions of the two silylenes with thiiranes, which afford products consistent with the formation of the corresponding transient silanethiones ($Me_2Si{=}S$ and $Ph_2Si{=}S$) along with the corresponding alkene, in chemical yields of 33−65%. Various aspects of the reactivity of $Me_2Si{=}S$ have been reported previously under high-temperature thermolytic conditions,[73,74,78] where the species dimerizes to the corresponding cyclodisilthiane (**16**) or can be trapped by added D_3 as the insertion product (**7**). Our experiments indicate that D_3 is also a reasonably effective trapping agent for $Me_2Si{=}S$ at ambient temperatures in solution, though the yield of **7** in this experiment was only half that of the propene produced; we could find no evidence for the formation of the silanethione dimer (**16**) by ^{1}H NMR spectroscopy[78] or GC/MS. In contrast, the oligosiloxane is a completely ineffective trapping agent for the diphenyl analog ($Ph_2Si{=}S$), whose main fate is dimerization to the corresponding cyclodisilthiane (**12**) both in the absence and presence of 0.2 M D_3. As expected, however,[42,43] the silanethione can be trapped efficiently by MeOH to afford the corresponding methoxysilanethiol (**15**), even at quite low concentrations (∼5 mM) of added alcohol. As with the photolyses in the presence of PrO and CHO, the chemical yields of alkene and silanethione-derived products obtained in the experiments with **1** and **2** in the presence of PrS are significantly less than 100%, and we were similarly unsuccessful in detecting the bulk of the missing material.

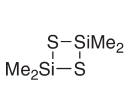

16

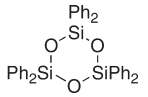

17

Goure and Barton also reported (isolated) material balances in the range of 40−50% in their study of the reaction of thermally- and photochemically generated $SiMe_2$ with cyclooctene oxide.[10] In the present cases, several minor molecular products were evident in each case in the GC/MS chromatograms of the crude photolyzates, but in no case did any of them stand out as being particularly prominent. We suspect that polymerization processes account for at least some of the deficiency in the material balance, though definitive signs of this were observed (by NMR) in only two instances: the photolysis of **2** in the presence of PrO with and without added D_3. Interestingly, comparison of the NMR spectra of these photolyzates to those of an authentic sample of the anticipated product of $Ph_2Si{=}O$ oligomerization, hexaphenylcyclotrisiloxane (**17**), demonstrated that it was not formed in appreciable yield under the conditions of these experiments.

The laser photolysis experiments show conclusively that the reactions of both $SiMe_2$ and $SiPh_2$ with CHO, PrO, and PrS proceed via multistep mechanisms involving the initial formation of the corresponding Lewis acid−base complexes, which have been detected as discrete intermediates that are formed on the same time scale as the decay of the free silylenes and subsequently decay with first-order kinetics. The complexes have been identified on the basis of their UV absorption spectra, which are indistinguishable from those of the corresponding silylene−THF[65,71,72] and silylene−THT complexes (Figures S4, S10

dx.doi.org/10.1021/ja107881p | J. Am. Chem. Soc. 2011, 133, 4377–4388

and ref 72) in each case. The absolute rate constants for formation of the complexes, as given by the rate constants for quenching of the free silylenes by the substrates, all lie within a factor of 2 of the diffusional rate constant in hexanes at 25 °C; they are consistently close to a factor of 2 larger for $SiMe_2$ than for $SiPh_2$, as usual,[65] but do not vary with the identity of the *O*- or *S*-donor. This indicates that complexation is an essentially barrierless process in all cases. The comparison of the optical yields of the $SiPh_2$−CHO and $SiPh_2$−THF complexes under equivalent conditions (vide supra) allows the conclusion that at substrate concentrations of 10 mM, complexation is the exclusive reaction of the free silylene with CHO. This is an important point, as it indicates that the deficiency in material balance that characterizes the steady state photolysis experiments must be due to competing decomposition channels of either the complex or a second reactive intermediate that is formed from the complex, and not to a second primary reactive process involving $SiPh_2$ and CHO that competes with complexation and which leads to products other than the alkene and silanone. It seems reasonable to assume that this is also true at the higher substrate concentrations employed in the product studies, and that it applies as well to the reactions of the other substrates with both $SiPh_2$ and $SiMe_2$; lifetime quenching of these silylenes by CHO, PrO and PrS proceeds with essentially the same rate constants as those for quenching by the corresponding "non-reactive" ether and sulfide substrates, THF and THT, respectively, whose interactions with $SiMe_2$ and $SiPh_2$ are confined to Lewis acid−base complexation and no further reaction involving the substrate ensues.

The absorbance versus time behavior observed for the two silylenes in the presence of submillimolar concentrations of each of these substrates is consistent with equilibrium constants for complexation in excess of $K_{cplx} > 30\,000\ M^{-1}$ in all cases, which corresponds to a standard free energy value of $\Delta G^\circ \leq -4.2$ kcal mol^{-1}, where the standard state is the gas phase at 1 atm pressure and 298.15 K. Calculated free energies of complexation of SiH_2 with oxirane and THF[19] lead to the expectation of somewhat larger equilibrium constants for complexation with THF and THT than with the oxiranes and PrS, respectively, but they are all larger than we can measure by our methods so the prediction cannot be verified experimentally, at least at room temperature. The B3LYP calculations predict a slightly more favorable free energy of complexation for $SiMe_2$ with thiirane than with oxirane, though they underestimate the stabilities of the complexes by at least 5−7 kcal mol^{-1} relative to our experimentally estimated upper limit of $\Delta G^\circ \leq -4.2$ kcal mol^{-1}. The experimental data afford no indication of the relative Lewis acidities of $SiMe_2$ and $SiPh_2$ toward the O- or S-donors; we note, however, that the equilibrium constants for complexation of the corresponding germylene derivatives ($GeMe_2$ and $GePh_2$) with THF and alcohols indicate that the phenylated derivative is significantly more acidic than the methylated one, the values being consistent with differences in free energy of complexation on the order of ca. 0.5 kcal mol^{-1} in hexanes at 25 °C.[81]

In keeping with their role as the first-formed intermediates in the O- and S-transfer reactions, the kinetic behavior exhibited by the silylene−PrO, −CHO, and −PrS complexes is distinctly different than that of the corresponding nonreactive complexes with THF and THT. The latter are quite long-lived, decaying over several tens of microseconds with second-order kinetics and the concomitant formation of the corresponding silylene dimers, Si_2Me_4 and Si_2Ph_4. On the other hand, the oxirane- and thiirane-complexes decay with clean first-order kinetics, *without* the concomitant formation of the corresponding disilenes, indicating that they each possess one or more low energy reaction channels that are absent in the complexes with THF and THT. The first-order rate coefficients for decay of the complexes are in each case independent of the concentration of the corresponding oxirane or thiirane, from which it can be concluded that they reflect the rates of *unimolecular* C−X bond cleavage, leading ultimately to the formation of alkene and silanone or silanethione in addition to other (unknown) products. As expected, there is no catalysis or reaction of the complexes that involves a second molecule of the substrate. The kinetic data, which are summarized in Table 1, reveal several distinct trends.

First, the k_{decay}-values for the oxirane complexes do not vary significantly as a function of substitution at silicon, indicating that differences in the steric and electronic properties of the methyl and phenyl substituents have a minimal impact on the rate constant for reaction of the silylene−oxirane complexes; on the other hand, dissociation of the two silylene−CHO complexes is roughly 35% faster than that of the silylene−PrO complexes. The rate constants correspond to effective free energies of activation ($\Delta G^{\ddagger}$) of 8.4−8.5 kcal mol^{-1} for the reaction(s) responsible for their decay. The calculated free energy of activation for C−O bond cleavage in the $SiMe_2$−oxirane complex, relative to the lower energy (anti-) conformer, is 8.1 kcal mol^{-1} (see Table 3). Methyl-substitution in the ring may lead to a slight lowering of the activation energy for C−O bond cleavage, but nevertheless, the calculated value for the parent oxirane−$SiMe_2$ complex is in quite reasonable agreement with the experimental values for the complexes with PrO and CHO in hexanes solution. Extrapolation of these considerations to the parent silylene suggests that the SiH_2−oxirane complex should possess a lifetime on the order of a few microseconds in the gas phase under conditions of complete vibrational relaxation.

In agreement with the ab initio calculations on the SiH_2−oxirane system (vide supra and ref 16), the present DFT calculations indicate that cleavage of the silylene−oxirane complexes proceeds in stepwise fashion from the gauche-conformer, yielding the corresponding (singlet) $R_2SiOCH_2CH_2$ biradical in the first step. The C−O bond that cleaves in this initial step is the one that bisects the silylene substituents in the gauche-complex, and the approach to the transition state involves only slight twisting about the developing Si−O bond; the main changes in geometry are a shortening of the Si−O bond distance, a substantial lengthening of the O−C1 distance, and slight shortening of the O−C2 and C1−C2 bond distances (C1 is defined as the carbon of the C−O bond that is cleaved; see Figure 5). Formation of the $H_2SiOCH_2CH_2$ biradical is predicted to be exergonic by ca. 13 kcal mol^{-1} at the UB3LYP/6-311+G(d,p) level of theory, in quite reasonable agreement with the value of ca. 10 kcal mol^{-1} that is predicted at the UQCISD/6-31G(d,p) level. An even greater exergonicity is predicted for the formation of the $Me_2SiOCH_2CH_2$ biradical—ca. 18 kcal mol^{-1} relative to the anti conformer of the complex—and a lower free energy of activation for its formation by ca. 2.5 kcal mol^{-1}. The theoretical prediction of exergonic biradical formation is consistent with the experimental rate constants for decomposition of the $SiMe_2$− and $SiPh_2$−PrO and CHO complexes. On the basis of silyl radical bond dissociation energies, one would expect phenyl substitution to lead to slightly greater stabilization of the $SiPh_2$-derived biradicals compared to those derived from $SiMe_2$;[82] the effect is small, but should nonetheless result in a faster rate of decomposition in the $SiPh_2$-complexes if the process is endergonic

Scheme 1

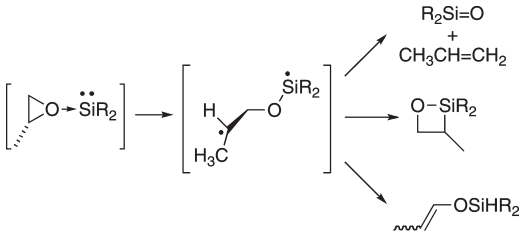

and the Hammond Postulate applies. The fact that essentially no difference in rate constant is observed suggests that biradical character is not substantially developed in the transition state for C−O bond cleavage, which is consistent with an exergonic process.

The somewhat faster rates of cleavage of the silylene−CHO complexes compared to those of the complexes with PrO is also consistent with the stepwise cleavage mechanism, assuming that the O−C bond to the more substituted carbon in PrO is the one preferentially cleaved in the initial step; all else being equal, one would expect cleavage of the complexes with the disubstituted oxirane derivative (CHO) to proceed with twice the rate constant exhibited by the PrO-complexes, based simply on statistical factors. The fact that the CHO-complexes react less than twice faster than the PrO-complexes could indicate that the enthalpic barrier for O−C bond cleavage is slightly higher for the disubstituted system, perhaps due to steric or strain-related factors.

Biradical involvement could also explain the low material balances observed in the steady-state photolysis experiments, since there are in principle at least two other modes of reaction possible for these species in addition to (the observed) β-cleavage to yield silanone and alkene: cyclization and 1,3-H migration to form the corresponding siloxetane and silyl enol ether, respectively (Scheme 1). Formation of these other products would in principle be possible if the dynamics of the biradical are appropriate, or if there is communication with the triplet state, which could lengthen the lifetime of the biradical to the point where conformational interconversion might be possible. Of the two additional potential products mentioned above, the silyl enol ethers should be most easily identifiable in the NMR spectra of the photolyzates, and we saw no evidence that they were formed. The possible competing formation of the corresponding siloxetanes is more difficult to rule out, though again we observed nothing that definitively suggested their presence in the NMR spectra. Neither product type would be expected to be detectable by GC/MS, though both should be sufficiently stable at room temperature in solution to be detected by NMR, if they were formed. While the present calculations suggest that the biradical is formed in a conformation that should favor β-cleavage over the other possible reaction pathways, higher levels of theory will be required in order to model its reactivity in a reasonably reliable way.

Dissociation of the silylene−PrS complexes proceeds significantly more rapidly than in the corresponding silylene−PrO complexes, and there is a distinct effect of silyl substituent on the rate constant. The decay of the $SiMe_2$−PrS complex is too fast to be resolved from our laser pulse, so only a lower limit of $k_{decay} \geq 4 \times 10^7\ s^{-1}$ could be obtained in this case and the quality of the spectrum obtained for the species (Figure S3b) is consequently rather poor; nevertheless, the spectrum compares reasonably well with that of the $SiMe_2$−THT complex (Figure S4b). A better spectrum has been obtained for the longer-lived $SiPh_2$−PrS complex (dashed line, Figure 3), which compares very well with that of the THT-derived species (Figure S10). The $SiPh_2$−PrS complex decays with a first-order rate constant of $k_{decay} \approx 2 \times 10^7\ s^{-1}$, corresponding to a free energy of activation of $\Delta G^{\ddagger} \approx 7.4$ kcal mol^{-1} for the reaction(s) responsible for its decay. A similar treatment of the data for the $SiMe_2$−PrS complex leads to a corresponding estimated upper limit of $\Delta G^{\ddagger} \leq 7.1$ kcal mol^{-1}. The calculated value of $\Delta G^{\ddagger} = 5.7$ kcal mol^{-1} for reaction of the $SiMe_2$−thiirane complex is consistent with this upper limit.

The variation in the decay rate constants for decay of the $SiMe_2$− and $SiPh_2$−PrS complexes contrasts the behavior observed for the silylene−oxirane complexes and suggests a different mechanism for their reaction, as indeed the calculations predict. The consistently faster rates of decay of the PrS complexes compared to the PrO- and CHO-complexes are also consistent with the results of the DFT calculations, which predict lower free energy barriers for reaction of both the SiH_2− and $SiMe_2$−thiirane complexes compared to those of the corresponding complexes with oxirane. The difference in the free energies of activation for decay of the $SiMe_2$− and $SiPh_2$−PrS complexes is consistent with a greater degree of exergonicity in the dissociation of the $SiMe_2$-complex compared to the phenylated system. Indeed, the calculated (B3LYP/6-311G(d)) values of the overall free energies for formation of ethylene and $Me_2Si{=}S$ and $Ph_2Si{=}S$ from thiirane and the corresponding silylenes are −52.4 and −49.5 kcal mol^{-1}, respectively (see Table S2). Steric factors may also contribute to some extent, as the calculations indicate that compared to the situation with the silylene-oxirane systems, a greater degree of twisting about the developing Si−S bond is required to achieve the transition state from the gauche conformer of the SiR_2−thiirane complex. This results in a transition state structure in which one of the silylene substituents is in a near-eclipsed arrangement with one of the C−S bonds in the thiirane ring.

Finally, the present study has allowed the transient silanethione $Ph_2Si{=}S$ to be detected directly and some aspects of its reactivity in solution to be studied for the first time. The species exhibits an intense ($\pi \rightarrow \pi^*$) absorption band and (apparently) a second very weak band centered at $\lambda_{max} \approx 275$ and 460 nm, respectively, in reasonable agreement with the theoretically predicted spectrum. If the 460 nm band is indeed due to the $n \rightarrow \pi^*$ absorption in $Ph_2Si{=}S$, it is red-shifted by ca. 65 nm relative to that reported by Tokitoh and co-workers for the sterically stabilized diarylsilanethione **18** (λ_{max} = 396 nm, ε = 100).[41] The parent diarylsilanethione undergoes rapid ($2k/\varepsilon_{290\text{-nm}} = (2.3 \pm 0.2) \times 10^6$ cm s^{-1}) head-to-tail dimerization as its primary mode of decay in the absence of reactive substrates; the rate coefficient corresponds to a value of $k_{dim} \approx 1 \times 10^{10}$ M^{-1}s^{-1} assuming a value of ca. 10 000 dm mol^1 cm^{-1} for the extinction coefficient at 290 nm. As expected, based on the behavior of other silanethiones that have been reported,[37,42,43] the species reacts rapidly with nucleophilic substrates such as aliphatic alcohols, acetic acid, and n-butyl amine, with rate constants that vary in more or less the expected manner with variations in substrate acidity, nucleophilicity, and steric bulk throughout the limited series of substrates that have been studied. One interesting point of comparison that can be made is with 1,1-diphenylsilene ($Ph_2Si{=}CH_2$), which reacts with the same substrates in hydrocarbon solvents with rate constants that are of similar magnitudes to those obtained for the silanethione

under similar conditions, and which vary in a similar way as a function of substrate structure.[83,84] Both species also undergo head-to-tail dimerization at close to the diffusion-controlled rates in the absence of added substrates.[85,86]

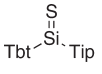

Tbt = 2,4,6-tris[bis(trimethylsilyl)methyl]phenyl
Tip = 2,4,6-triisopropylphenyl

18

SUMMARY AND CONCLUSIONS

The transient silylenes $SiMe_2$ and $SiPh_2$ react rapidly, albeit with only ca. 50% overall efficiency, with simple oxirane and thiirane derivatives in solution to afford the corresponding transient silanones and silanethiones, respectively. These reactions have been shown to proceed via multistep mechanisms involving the initial, barrierless formation of the corresponding silylene−substrate Lewis acid−base complex, from which the net X-atom transfer reaction proceeds. The complexes have been detected directly and the rate constants for the rate-controlling step in their unimolecular decomposition have been determined. The experimental data are consistent with theoretical predictions of a stepwise process involving biradical intermediates for the reaction of the silylene−oxirane complexes, and concerted S-atom transfer in the case of the silylene−thiirane complexes. Diphenylsilanethione, the product of S-atom transfer from propylene sulfide to diphenylsilylene, has been detected directly for the first time, and absolute rate constants have been reported for its head-to-tail dimerization and its reactions with methanol, *tert*-butanol, acetic acid, and *n*-butyl amine in hexanes solution at 25 °C. The UV−vis spectrum exhibited by the species under these conditions agrees well with that predicted by TD-DFT calculations at the B3LYP/6-311G(d) level of theory.

While it is clear that other detection methods will need to be employed for the study of the other transient silicon-chalcogen doubly bonded species implicated in this work, our results demonstrate that O- and S-transfer reactions with transient silylenes represent a potentially quite powerful method for the generation of these elusive species for study in solution. Further work in this direction, as well as more detailed mechanistic studies of these reactions, is in progress.

EXPERIMENTAL SECTION

Details pertaining to the synthesis and characterization of the silylene precursors and reaction products, steady state and laser flash photolysis experiments, and computational studies are given in the Supporting Information.

ASSOCIATED CONTENT

Supporting Information. Details of the preparation and characterization of compounds; additional kinetic data determined in laser flash photolysis experiments; NMR spectra and concentration vs time plots from steady state photolysis experiments; details of the computational study and tables of calculated Cartesian coordinates and energies. This material is available free of charge via the Internet at http://pubs.acs.org.

AUTHOR INFORMATION

Corresponding Author
leigh@mcmaster.ca

ACKNOWLEDGMENT

We thank the Natural Sciences and Engineering Research Council of Canada for financial support for this work, and Drs. N. H. Werstiuk and P. Ayers for helpful advice and discussion. Part of this work was made possible by the facilities of the Shared Hierarchical Academic Research Computing Network (SHARCNET:www.sharcnet.ca) and Compute/Calcul Canada.

REFERENCES

(1) Gaspar, P. P. In *Reactive Intermediates*, Vol. 1; Jones, M., Jr., Moss, R. A, Eds.; John Wiley & Sons: New York, 1978; pp 229−277.
(2) Gaspar, P. P.; West, R. In *The Chemistry of Organic Silicon Compounds*, Vol. 2;Rappoport, Z., Apeloig, Y., Eds.; John Wiley & Sons: New York, 1998; pp 2463−2568.
(3) Tokitoh, N.; Ando, W. In *Reactive Intermediate Chemistry*; Moss, R. A., Platz, M. S., Jones, M., Jr., Eds.; John Wiley & Sons: New York, 2004; pp 651−715.
(4) Kirmse, W. In *Advances in Carbene Chemistry*; Brinker, U. H., Ed.; Elsevier: Amsterdam, 2001; Vol. 3, pp 1−51.
(5) Leigh, W. J.; Kostina, S. S.; Bhattacharya, A.; Moiseev, A. G. *Organometallics* **2010**, *29*, 662.
(6) Du, X. M.; Fan, H.; Goodman, J. L.; Kesselmayer, M. A.; Krogh-Jespersen, K.; LaVilla, J. A.; Moss, R. A.; Shen, S.; Sheridan, R. S. *J. Am. Chem. Soc.* **1990**, *112*, 1920.
(7) Pliego, J. R., Jr.; De Almeida, W. B. *J. Phys. Chem. A* **1999**, *103*, 3904.
(8) Jutzi, P.; Bunte, E. A. *Angew. Chem., Int. Ed.* **1992**, *31*, 1605.
(9) Muller, T.; Jutzi, P.; Kuhler, T. *Organometallics* **2001**, *20*, 5619.
(10) Goure, W. F.; Barton, T. J. *J. Organomet. Chem.* **1980**, *199*, 33.
(11) Tzeng, D.; Weber, W. P. *J. Am. Chem. Soc.* **1980**, *102*, 1451.
(12) Ando, W.; Ikeno, M.; Hamada, Y. *Chem. Commun.* **1981**, 621.
(13) Arrington, C. A.; West, R.; Michl, J. *J. Am. Chem. Soc.* **1983**, *105*, 6176.
(14) Barton, T. J. *Pure Appl. Chem.* **1980**, *52*, 615.
(15) Baggott, J. E.; Blitz, M. A.; Frey, H. M.; Lightfoot, P. D.; Walsh, R. *Int. J. Chem. Kinet.* **1992**, *24*, 127.
(16) Apeloig, Y.; Sklenak, S. *Can. J. Chem.* **2000**, *78*, 1496.
(17) Su, M. D. *J. Phys. Chem. A* **2002**, *106*, 9563.
(18) Su, M. D. *J. Am. Chem. Soc.* **2002**, *124*, 12335.
(19) Becerra, R.; Cannady, J. P.; Goulder, O.; Walsh, R. *J. Phys. Chem. A* **2010**, *114*, 784.
(20) Nozaki, H.; Takaya, H.; Noyori, R. *Tetrahedron* **1966**, *22*, 3393.
(21) Shields, C. J.; Schuster, G. B. *Tetrahedron Lett.* **1987**, *28*, 853.
(22) Pezacki, J. P.; Wood, P. D.; Gadosy, T.; Lusztyk, J.; Warkentin, J. *J. Am. Chem. Soc.* **1998**, *120*, 8681.
(23) Hata, Y.; Watanabe, M.; Inoue, S.; Oae, S. *J. Am. Chem. Soc.* **1975**, *97*, 2553.
(24) Raabe, G.; Michl, J. *Chem. Rev.* **1985**, *85*, 419.
(25) Maltsev, A. K.; Khabashesku, V. N.; Nefedov, O. M.; Zelinsky, N. D. In *Silicon Chemistry*; Corey, E. Y., Corey, J. Y., Gaspar, P. P., Eds.; Ellis Horwood: Chichester, 1988; pp 211−223.
(26) Apeloig, Y. In *The Chemistry of Organic Silicon Compounds*; Patai, S., Rappoport, Z., Eds. Wiley: Chichester, U.K., 1989; Chapter 2.
(27) Tokitoh, N.; Okazaki, R. In *The Chemistry of Organic Silicon Compounds*; Rappoport, Z., Apeloig, Y., Eds.; John Wiley & Sons Ltd.: New York, 1998; pp 1063−1103.
(28) Takeda, N.; Tokitoh, N.; Okazaki, R. *Chem. Lett.* **2000**, 244.
(29) Takeda, N.; Tokitoh, N. *Synlett* **2007**, 2483.
(30) Yao, S.; Brym, M.; van Wüllen, C.; Driess, M. *Angew. Chem., Int. Ed.* **2007**, *46*, 4159.
(31) Yao, S.; Xiong, Y.; Brym, M.; Driess, D. *J. Am. Chem. Soc.* **2007**, *129*, 7268.
(32) Xiong, Y.; Yao, S.; Driess, M. *J. Am. Chem. Soc.* **2009**, *131*, 7562.
(33) Xiong, Y.; Yao, S.; Muller, R.; Kaupp, M.; Driess, M. *Nat. Chem.* **2010**, *2*, 577.
(34) Xiong, Y.; Yao, S.; Driess, M. *Dalton Trans.* **2010**, *39*, 9282.

(35) Xiong, Y.; Yao, S.; Driess, M. *Angew. Chem., Int. Ed.* **2010**, *49*, 6642.
(36) Yao, S.; Xiong, Y.; Driess, M. *Chem.—Eur. J.* **2010**, *16*, 1281.
(37) Arya, P.; Boyer, J.; Carre, F.; Corriu, R.; Lanneau, G.; Lapasset, J.; Perrot, M.; Priou, C. *Angew. Chem., Int. Ed. Engl.* **1989**, *28*, 1016.
(38) Yao, S.; Yun, X.; Brym, M.; Driess, M. *Chem. Asian J.* **2008**, *3*, 113.
(39) Epping, J. D.; Yao, S.; Karni, M.; Apeloig, Y.; Driess, M. *J. Am. Chem. Soc.* **2010**, *132*, 5443.
(40) Haaf, M.; Schmiedl, A.; Schmedake, T. A.; Powell, D. R.; Millevolte, A. J.; Denk, M.; West, R. *J. Am. Chem. Soc.* **1998**, *120*, 12714.
(41) Suzuki, H.; Tokitoh, N.; Nagase, S.; Okazaki, R. *J. Am. Chem. Soc.* **1994**, *116*, 11578.
(42) Suzuki, H.; Tokitoh, N.; Okazaki, R.; Nagase, S.; Goto, M. *J. Am. Chem. Soc.* **1998**, *120*, 11096.
(43) Iwamoto, T.; Sato, K.; Ishida, S.; Kabuto, C.; Kira, M. *J. Am. Chem. Soc.* **2006**, *128*, 16914.
(44) Kira, M. *Chem. Commun.* **2010**, *46*, 2893.
(45) Withnall, R.; Andrews, L. *J. Am. Chem. Soc.* **1986**, *108*, 8118.
(46) Khabashesku, V. N.; Kerzina, Z. A.; Baskir, E. G.; Maltsev, A. K.; Nefedov, O. M. *J. Organomet. Chem.* **1988**, *347*, 277.
(47) Korolev, V. A.; Nefedov, O. M. *Adv. Phys. Org. Chem.* **1995**, *30*, 1.
(48) Khabashesku, V. N.; Kerzina, Z. A.; Kudin, K. N.; Nefedov, O. M. *J. Organomet. Chem.* **1998**, *566*, 45.
(49) Maier, G.; Meudt, A.; Jung, J.; Pacl, H. In *The Chemistry of Organic Silicon Compounds*; Rappoport, Z., Apeloig, Y., Eds.; John Wiley & Sons: New York, 1998; pp 1143−1185.
(50) Khabashesku, V. N.; Kudin, K. N.; Margrave, J. L.; Fredin, L. *J. Organomet. Chem.* **2000**, *595*, 248.
(51) Kudo, T.; Nagase, S. *J. Am. Chem. Soc.* **1985**, *107*, 2589.
(52) Schmidt, M. W.; Truong, P. N.; Gordon, M. S. *J. Am. Chem. Soc.* **1987**, *109*, 5217.
(53) Gordon, M. S.; Pederson, L. A. *J. Phys. Chem.* **1990**, *94*, 5527.
(54) Kapp, J.; Remko, M.; Schleyer, P. v. R. *Inorg. Chem.* **1997**, *36*, 4241.
(55) Galbraith, J. M.; Blank, E.; Shaik, S.; Hiberty, P. C. *Chem.—Eur. J.* **2000**, *6*, 2425.
(56) Kimura, M.; Nagase, S. *Chem. Lett.* **2001**, 1098.
(57) Avakyan, V. G.; Sidorkin, V. F.; Belogolova, E. F.; Guselnikov, S. L.; Gusel'nikov, L. E. *Organometallics* **2006**, *25*, 6007.
(58) Sheu, J.-H.; Su, M.-D. *Organometallics* **2010**, *29*, 527.
(59) Kudo, T.; Nagase, S. *Organometallics* **1986**, *5*, 1207.
(60) Köppe, R.; Schnöckel, H. *Z. Anorg. Allg. Chem.* **1992**, *607*, 41.
(61) Guimon, C.; Pfister-Guillouzu, G.; Lavayssiere, H.; Dousse, G.; Barrau, J.; Satge, J. *J. Organomet. Chem.* **1983**, *249*, C17.
(62) Lefevre, V.; Ripoll, J.-L. *Phosphorus, Sulfur Silicon* **1997**, *120*−*121*, 371.
(63) Chrostowska, A.; Joanteguy, S.; Pfister-Guillouzo, G. *Organometallics* **1999**, *18*, 4795.
(64) Moiseev, A. G.; Leigh, W. J. *Organometallics* **2007**, *26*, 6268.
(65) Moiseev, A. G.; Leigh, W. J. *Organometallics* **2007**, *26*, 6277.
(66) Ishikawa, M.; Kumada, M. *Adv. Organomet. Chem.* **1981**, *19*, 51.
(67) Tortorelli, V. J.; Jones, M., Jr.; Wu, S.; Li, Z. *Organometallics* **1983**, *2*, 759.
(68) Michalczyk, M. J.; Fink, M. J.; De Young, D. J.; Carlson, C. W.; Welsh, K. M.; West, R.; Michl, J. *Silicon, Germanium, Tin Lead Compd.* **1986**, *9*, 75.
(69) Miyazawa, T.; Koshihara, S. Y.; Liu, C.; Sakurai, H.; Kira, M. *J. Am. Chem. Soc.* **1999**, *121*, 3651.
(70) Leigh, W. J.; Moiseev, A. G.; Coulais, E.; Lollmahomed, F.; Askari, M. S. *Can. J. Chem.* **2008**, *86*, 1105.
(71) Levin, G.; Das, P. K.; Bilgrien, C.; Lee, C. L. *Organometallics* **1989**, *8*, 1206.
(72) Yamaji, M.; Hamanishi, K.; Takahashi, T.; Shizuka, H. *J. Photochem. Photobiol., A* **1994**, *81*, 1.
(73) Soysa, H. S. D.; Jung, I. N.; Weber, W. P. *J. Organomet. Chem.* **1979**, *171*, 177.
(74) Soysa, H. S. D.; Weber, W. P. *J. Organomet. Chem.* **1979**, *165*, C1.
(75) Soysa, H. S. D.; Okinoshima, H.; Weber, W. P. *J. Organomet. Chem.* **1977**, *133*, C17.
(76) Teng, C. J.; Weber, W. P.; Cai, G. *Polymer* **2003**, *44*, 4149.
(77) Mayfield, D. L.; Flath, R. A.; Best, L. R. *J. Org. Chem.* **1964**, *29*, 2444.
(78) Sommer, L. H.; McLick, J. *J. Organomet. Chem.* **1975**, *101*, 171.
(79) Lee, C.; Yang, W.; Parr, R. G. *Phys. Rev. B* **1988**, *37*, 785.
(80) Becke, A. D. *J. Chem. Phys.* **1993**, *98*, 5648.
(81) Leigh, W. J.; Lollmahomed, F.; Harrington, C. R.; McDonald, J. M. *Organometallics* **2006**, *25*, 5424.
(82) Walsh, R. *Acc. Chem. Res.* **1981**, *14*, 246.
(83) Bradaric, C. J.; Leigh, W. J. *Can. J. Chem.* **1997**, *75*, 1393.
(84) Leigh, W. J.; Li, X. *J. Phys. Chem. A* **2003**, *107*, 1517.
(85) Toltl, N. P.; Stradiotto, M. J.; Morkin, T. L.; Leigh, W. J. *Organometallics* **1999**, *18*, 5643.
(86) Morkin, T. L.; Leigh, W. J. *Organometallics* **2001**, *20*, 4537.